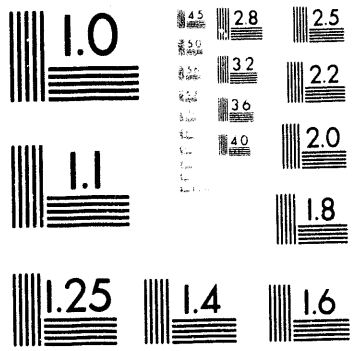
1.0
1.1
1.25
1.4
1.6
1.8
2.0
2.2
2.5
2.8
3.2
3.6
4.0
4.5
5.0

1 of 1

ANL/CHM/CP--81119

STUDIES OF THIN-FILM GROWTH, ADSORPTION, AND OXIDATION BY IN SITU, REAL-TIME, AND EX SITU ION BEAM ANALYSIS

Yuping Lin[1,2], A. R. Krauss[1], O. Auciello[3], Y. Niahino[1,4], D. M. Gruen[1], R. P. H. Chang[2], and J. A. Schultz[5]

[1]Materials Science and Chemistry Divisions, Argonne National Laboratory, Argonne, IL 60439
[2]Department of Materials Science, Northwestern University, Evanston, IL 60208
[3]MCNC, Electronics Technology Division, Research Triangle Park, NC 27709
[4]Hitachi Central Research Laboratory, Hitachi City, Japan
[5]Ionwerks, Houston, TX 71310

To be presented at the

40th National Symposium of the American Vacuum Society, Orlando, FL
November 15-19, 1993

*Work supported by the U.S. Department of Energy, BES-Materials Sciences, under Contract W-31-109-ENG-38, as part of a cooperative research and development agreement between Argonne National Laboratory and the Ionwerks Corporation; and the Advanced Research Programs Agency under Grant N00014-93-0591.

to be presented at the 40th National Symposium of the American Vacuum Society, Orlando FL November 15-19, 1993

STUDIES OF THIN-FILM GROWTH, ADSORPTION, AND OXIDATION BY IN SITU, REAL-TIME, AND EX SITU ION BEAM ANALYSIS

Yuping Lin[1,2], A. R. Krauss[1], O. Auciello[3], Y. Nishino[1,4], D. M. Gruen[1], R. P. H. Chang[2], and J. A. Schultz[5]

1 Materials Science and Chemistry Divisions, Argonne National Laboratory, Argonne, IL 60439
2 Department of Materials Science, Northwestern University, Evanston, IL 60208
3 MCNC, Electronics Technology Division, Research Triangle Park, NC 27709
4 Hitachi Central Research Laboratory, Hitachi City, Japan
5 Ionwerks Inc., Houston, TX 71310

We have developed a time-of-flight (TOF) ion scattering and direct recoil spectrometer (ISS/DRS) to study the surface composition and reconstruction of metals, metal-oxides, and semiconductors, and to provide in situ characterization of the thin-film deposition process. The in situ, real-time study of Pb, Zr, and Ru ultrathin films produced by ion beam sputter deposition is presented here as the first demonstration of pulsed ion beam surface analysis (PIBSA) as a means of characterizing monolayer and submonolayer growth, both in UHV and in mTorr oxygen background. The capability of performing surface analysis at pressures $>10^{-3}$ Torr is unique to pulsed ion beam surface analysis among surface analytical methods and enables the in situ monitoring of oxide thin-film growth processes and surface-gas phase reactions. Using angular-resolved ISS (ARISS), combined with Auger electron spectroscopy (AES), we studied the oxygen adsorption and reconstruction of (001) oriented InSb thin-film surfaces. It was found that the adsorption of molecular oxygen on the InSb (001) surface is consistent with the Langmuir model. Oxygen adsorption preferentially occurs on the antimony sites corresponding to the extension of the lattice into the vacuum and reduces the inward contraction of the first two layers of the clean InSb (001) surface relative to the bulk atomic spacing.

I. INTRODUCTION

The interaction of material surfaces with the atmosphere, especially oxygen, is a very important topic in surface science and materials research because of its role in materials synthesis, particularly the formation of oxides, the effects on the characteristics of multilayer interfaces, and the influence on electronic device performance. The fabrication of multicomponent oxide films, such as high-temperature superconductors and ferroelectric materials, is usually carried out in an atmosphere consisting of oxygen at a partial pressure of several mTorr. Most surface-analytical

techniques, however, are restricted to ultrahigh vacuum conditions. Time-of-flight ion scattering and direct recoil spectrometers (ISS/DRS)[1,2,3] have also been traditionally applied to determination of surface structure and composition under UHV conditions. We have developed an ISS/DRS spectrometer with differentially pumped detectors for the in situ study of surface adsorption and oxidation, as well as thin-film deposition, in relatively high (mTorr range) background gas pressure environments.

For many device applications, it is necessary to control the film properties at extremely sharp interfaces and to verify the integrity of layers whose thicknesses approach that of the atomic layer spacing. This requires analytical techniques that are able to characterize the uppermost 1-2 atomic layers of a growing thin-film in situ. Additionally, the system we have developed is physically compatible with existing thin-film deposition technologies. Low-energy, pulsed ion beam surface analysis is unique in that it is the only surface analytical method with depth resolution < 10 Å that can be used at ambient pressure > 10^{-6} Torr. Two examples of this capability are presented, corresponding to: (1) in situ monitoring of Pb and Ru deposition as a preliminary study directed at investigation of the behavior of depositing species relevant to the synthesis of ferroelectric $Pb(Zr_xTi_{1-x})O_3$ (PZT) films and RuO_2 contact layers, and (2) surface structure determination for oxygen adsorption on InSb.

PZT is of potential use in ferroelectric nonvolatile memories. However, the growth of PZT films is complicated by the fact that Pb is highly volatile at the temperatures needed to produce the PZT phase, requiring an oxygen background during deposition to stabilize Pb in the film. For PZT film-based capacitors used in nonvolatile memories, there is also a problem related to the interfaces between the PZT and the top and bottom contact layers. Capacitors with Pt electrodes are subject to polarization fatigue after ~10^6 polarization reversals. Various models suggest that oxygen vacancies located at or near the interface between the PZT and the electrode material are responsible for the fatigue mechanism, and it has been demonstrated that the use of conducting oxide electrodes such as RuO_2[4] or $La_{0.5}Sr_{0.5}CoO_3$[5,6] greatly reduces or eliminates fatigue. PIBSA offers the possibility of characterizing the processes occurring during growth of the PZT layer and at the PZT-electrode interface. In addition, PIBSA can be used to characterize other ferroelectric-based heterostructure interfaces.

The compound semiconductor InSb is a technologically promising material because of its small electron effective mass and narrow band gap.[7] The ability to grow high-quality epitaxial films is directly linked to surface or interface compositional and structural phenomena, such as surface segregation, contamination, and reconstruction.[8] Compared to the (110) surfaces of the zinc-blende materials that can be prepared simply by cleavage in vacuum, the technologically more important (001) surfaces have to undergo methods of sample preparation more likely to induce structural damage or changes in the surface stoichiometry.[9] Previous studies have used reflection

electron diffraction (RED),[10] low-energy electron diffraction (LEED), and scanning tunneling microscopy (STM)[8] to characterize clean "stabilized" c(8x2) surfaces, using protective overlayer techniques for preparation of InSb (001) surfaces,[11] and thermal desorption to remove InSb surface oxides.[12] However, an in situ investigation of the oxygen adsorption process has not yet been made. From a technological point of view, a clear understanding of surface reactions not only helps to prevent unwanted surface contamination and interface degradation, but also builds the foundation for the development of oxide layer growth methods in the fabrication of semiconductor devices. The second point is one of the key issues to be resolved before III-V semiconductors can replace silicon in device applications. Our experimental results show that TOF-ISS is one of the most powerful tools to study the surface adsorption and reconstruction of compound semiconductors.

II. EXPERIMENTAL

The experimental apparatus is shown schematically in Fig.1. It consists of an UHV surface analysis chamber with ISS/DRS and an Auger electron spectrometer, coupled to a multitarget ion beam sputter-deposition system through a 6 mm differential pumping aperture. The base pressure of the analysis chamber is in the 10^{-9} Torr range. Oxygen gas can be introduced into the chamber through a leak valve for adsorption studies. The detailed description of the ISS/DRS instrumentation has been published partially[13] and is described in greater detail in another paper in these proceedings.[14] The inert gas ion beam (normally set at 10 keV) is produced by an Atomika ion source and chopped into pulses 10-500 ns long by two sets of deflection plates and four apertures (which can be adjusted over the range 0.125-4 mm diameter). The ion beam is incident on the sample, which is located on the chamber axis, and is scattered at an angle of 165° into a channel electron multiplier detector. A second detector is positioned in the forward direction to detect direct recoil-ejected surface atoms.

For in situ, real-time surface analysis, we studied Pb and Ru submonolayer growth both at room temperature in high vacuum and under conditions corresponding to PZT thin-film nucleation and growth.[15] The films were grown by using a multitarget ion beam sputter-deposition system (IBSD) previously developed by Krauss and Auciello[16,17]. For the work reported here, a 4 keV, 1 mA Kr^+ ion beam was used to sputter Pb, Zr, and Ru targets. The sputtering chamber was held at 10^{-3}-10^{-4} Torr (of Kr gas), while the analysis chamber was in the range of 10^{-5} Torr, achieved by the differential pumping established by a 6 mm aperture between the two chambers. Because of the long distance between the targets and the substrate (~16 inches), the deposition rate is rather low (~0.2 Å/min for Pb deposition) but is sufficient for nucleation and initial growth studies. In order to calibrate the deposition rate, two quartz-crystal, thin-film deposition monitors, designated as QC1 and QC2 are mounted as shown in Fig. 1. QC1 is located in the deposition chamber and

continuously samples an atomic flux which is much higher than but proportional to the flux incident on the substrate. QC2 is positioned 2.7 cm above the center of the substrate and may be moved into the position normally occupied by the substrate for calibration purposes. Using a Pb target which provides a high deposition rate, it was found that the flux to the substrate was 200 times smaller than the flux to QC1.

In our experiments on InSb, a 10 keV Ar^+ beam of 10-50 ns pulse width and 1-2 mm in diameter was used for good mass resolution and low dose during analysis. The time-averaged pulsed beam current was ~10^{-10}A, and a typical spectrum was acquired in 50 seconds of beam time. Consequently, the accumulated primary ion dose was ~$1x10^{12}$ ions/cm^2 per acquired spectrum. Considering that there are ~10^{15} atoms/cm^2 on the surface of a typical solid, the beam dose causes negligible damage, even when a number of spectra are acquired at the same point on the sample surface, such as in the angle-resolved ISS (ARISS) study used to characterize the surface structure of InSb. InSb (001) films 1 μm thick grown by metalorganic vapor phase epitaxy (MOVPE)[18] on (001) GaSb substrates were used for the studies discussed in this paper. The orientation was determined by x-ray rocking curve diffraction and Laue diffraction.

III. RESULTS AND DISCUSSION

A. In Situ, Ultrathin-Film Growth Study

Figure 2a shows the 10 keV Ar^+ ISS spectra of a polycrystalline stainless steel foil used as the initial substrate material for deposition of Pb, Zr, and Ru at room temperature. In general, well-defined ISS peaks are not observed for surface species which are lighter than the primary ion beam. Since the substrate was initially covered by a hydrocarbon contamination layer, Fig. 2a shows only a broad background corresponding to multiple scattering of the primary ions and recoil emission from the hydrocarbon layer. Fig. 2b shows the ISS spectrum after depositing ~3.7 Å (1.2 ML) of Pb. An intense, symmetric Pb peak with a FWHM of 0.19 μsec is observed. It should be noted that scattering from an atomic species which is distributed in a layer more than one monolayer in thickness results in an asymmetric peak with a sharp rise on the short ToF side, and a long ToF tail resulting from multiple scattering events with second and third layer atoms. The observed Pb peak is symmetric, with a width which is consistent with the intrinsic resolution of the instrument and, therefore, corresponds to a single scattering event from a layer of Pb not exceeding one monolayer in thickness.[14] Figures 2c and 2d show the spectra after 1.2 Å and 2.9 Å layers of Ru, corresponding to 0.5 and 1.2 ML, respectively, were grown subsequent to the Pb deposition. The initial 0.5 ML deposition of Ru produces a decrease of only 6% in the Pb signal, while deposition of more than 1 ML of Ru results in a reduction of the Pb signal to 57% of the initial value as shown in Figure 2d. These results suggest that either (1) the initial sticking coefficient for Ru on Pb is very low, (2) Ru accumulates initially in thick islands covering only a small

portion of the surface, or (3) Pb segregates, covering the initial Ru almost as fast as it is deposited. The Ru peak is symmetric, and the measured FWHM of 0.35 μsec is consistent with the isotopic mass distribution, with principal isotopic abundances covering an atomic mass range of 99-104, indicating that little, if any, of the observed peak width is due to Ru island formation. A calculation of Pb segregation in Ru was performed using a procedure based on the Miedema model of binary alloys.[19] It was found that for a monolayer of Ru deposited on Pb, a complete exchange between the first and second atomic layers will occur, leaving the uppermost atomic layer consisting entirely of Pb. Such phenomena, of course, strongly influence the thin-film growth process and must be studied in greater detail.

Subsequent to the deposition of the Ru and Pb layers, as shown in Fig. 2, an additional Pb layer (~11Å thick, or 3.5 ML) was grown at room temperature in a Kr background pressure of 1.2×10^{-5} Torr (due to the gas loading from the sputtering chamber into the analysis chamber) on the surface represented by Fig. 2d (corresponding to ~0.57 ML Pb and ~0.43ML Ru). In situ, real-time ISS analysis was performed and the results are shown in Fig. 3. The Pb signal increases linearly in intensity for a period of time corresponding to the deposition of an additional 0.5 ML of Pb, as determined by the calibration of the quartz crystal monitor QC1. At this point, (~1 ML Pb, indicated by the letter b in Fig. 3), the growth rate of the Pb signal slows abruptly, indicating either that the Pb sticking coefficient is very small or that Pb is being deposited onto an underlying Pb layer, which does not give rise to an increase in signal because of the surface specificity of the ISS method. At point c, corresponding to a total Pb deposition of 2.0 ML, the Pb signal again starts to increase, leveling off at a total Pb dose corresponding to 3.0 ML (point d), again based on the calibration of the quartz crystal monitor QC1. The Pb signal intensity doubled in the region a-b when the Pb dose increased from 0.5 ML to 1 ML, corresponding to the condition in which each added Pb atom was as exposed to the primary beam as all previously deposited Pb atoms. In the region b-c (1-2 ML), each deposited Pb atom shadowed an underlying Pb atom, with the result that there was little change in the Pb signal. In the region c-d (2-3 ML), the signal increased by an additional 50%, suggesting a surface reconstruction in which the newly deposited Pb atoms only partly shield the previously deposited Pb atoms, and therefore, the scattering signal consists of components arising from approximately 50% of the second Pb layer as well as the uppermost layer of Pb atoms.

Figure 4 shows sequential 10keV Ne^+ ISS spectra taken during Pb deposition onto a Zr-covered RuO_2 film on a MgO substrate in an atmosphere of 5×10^{-4} Torr oxygen at an elevated substrate temperature. The peak corresponding to Zr has the asymmetric shape characteristic of a film several monolayers thick. Growth of Pb was not observed at temperatures above 420°C or at any temperature above 330°C in the absence of oxygen, demonstrating that oxygen is necessary to stabilize the Pb component in a growing PZT film. Successive spectra were taken at six-minute

intervals during deposition at 420°C, corresponding to incremental thickness increases of ~0.2Å and showing the continued growth of Pb as a single atomic layer with little or no tendency to form islands. Further studies to understand the growth of Pb, Zr, and Ti layers during PZT deposition are in progress.

B. Study of InSb Surface Adsorption and Oxidation

InSb (001) epitaxial thin-films were used to demonstrate the ability of ISS to determine surface structure in an ambient oxygen environment and to characterize the oxygen adsorption process. For comparison with the ISS results, oxygen adsorption on InSb (001) was also studied by AES using a double-pass cylindrical mirror Auger analyzer mounted in the ISS analysis chamber. Figure 5a is the Auger spectrum of an InSb (001) surface which has been cleaned by Ar^+ sputtering at room temperature. Because of the low melting point of InSb (525.7°C),[20] the surface maintains the zinc-blende lattice structure after sputter cleaning.[21] Spectrum 5b shows that after 60 minutes of exposure to oxygen at 10^{-6} Torr (3600 L), the Sb ($M_4N_{45}N_{45}$) and ($M_5N_{45}N_{45}$) peaks both decreased in intensity to nearly half of their initial value, suggesting that oxygen adsorbs preferentially on Sb lattice sites. If we assume that the Sb (MNN) line shape is uneffected by oxygen adsorption, this corresponds to an oxygen overlayer ~5Å thick. However, there is an increase in the In (MNN) peak-peak height in the dN/dE spectrum. Such effects are often due to an oxidation-induced change in the Auger line shape and constitute a source of ambiguity in using AES data to study adsorption of chemically active gases.

Figure 5c is the Auger spectrum of the sample of Figure 5b after 18 hours residence in a vacuum of $1x10^{-9}$ Torr. Compared to Fig. 5b which was taken immediately after a total O_2 exposure of 3600 L, the O (KLL) peak has decreased while the Sb (MNN) peaks have increased, suggesting either that the oxygen which adsorbed primarily on the Sb sites was partially desorbed when the oxygen ambient was removed, that Sb diffuses to the surface covering In sites and some of the adsorbed O sites, that the increasing C signal results from preferential adsorption of residual hydrocarbon on the oxygen sites, or some combination of the above.

The peak-peak intensity of the O(KLL) line is shown as a function of total O_2 exposure in Fig. 6. The oxygen exposure was carried out in 300 L increments at a pressure of $1x10^{-6}$ Torr. After 300 seconds of exposure, the oxygen was pumped out of the analysis chamber and an Auger spectrum was obtained. The result is consistent with the Langmuir model, indicating that the adsorption rate is proportional to the number of available adsorption sites: $dN/dt=kP(N_S-N)$, where dN/dt is the adsorption rate, N_S is the total number of sites, N is the number of occupied sites, t is the exposure time, P is the oxygen pressure, and k is the sticking coefficient. The number of Sb sites on the (001) InSb surface is $4.76x10^{14}/cm^2$, and we can calculate k from a plot of ln(Ns-N) against the exposure P*t. It is assumed that Ns-N is directly proportional to the AES intensity (I_S-

I), where I_S is the intensity corresponding to oxygen saturation of the adsorption sites. The resulting value for the sticking coefficient k for molecular oxygen on the InSb (001) surface at room temperature is 9.4×10^{-3}. This is high compared to the previously reported value[22] of 10^{-5}. One reason for the large measured value is that our sample was sputter-cleaned and contains a large number of defects which act as efficient adsorption sites. Additionally, the presence of CO in the ultrahigh vacuum apparatus and possible interaction between the primary electron beam and the adsorbed molecules can promote oxygen adsorption.[22]

Figure 7 shows sequential ISS spectra of InSb taken during oxygen exposure at a pressure of 1×10^{-6} Torr. Spectrum a shows the clean InSb (001) surface. Each following spectrum (b-g) was taken at ten minute intervals corresponding to incremental doses of 600 L up to a total dose of 3600 L. The intensity of the Sb peak decreases as the oxygen exposure increases, while the intensity of the In peak remains practically the same. This result is in agreement with the conclusion reached from the AES data that oxygen is preferentially adsorbed on top of the Sb atom sites.

The sample was then stored in a vacuum of 1×10^{-9} Torr for six days, followed by an automated ISS depth profile in which the ion beam was switched to dc operation for 1-minute intervals between successive data acquisition cycles. The dc beam consisted of 10 keV Ar^+ at a current density of 10^{-6} A/cm^2, resulting in a removal of ~0.5 monolayers between successive spectra. Before sputter cleaning (Fig. 8a), only a broad background signal is seen, corresponding to multiple scattering and recoil emission from adsorbed hydrocarbon species at the surface. With the removal of only 1 ML, the Sb peak is clearly seen (Fig. 8c), and the In signal is just starting to emerge from the noise. With further sputtering (Fig. 8d,e,f), the In intensity increases to a value almost equal to Sb intensity, supporting the hypothesis that the surface atomic layer tends to be Sb-rich, perhaps because of oxygen-induced Sb segregation.

InSb has the zinc-blende structure.[2] For polar ARISS along the [010] azimuth, the alternate Sb rows and In rows are parallel to both the incident and scattered beam directions (as show in the inset at the top of Fig. 9). The figure only shows an Sb plane, which is in the plane of paper, while two adjacent In planes above and beneath the plane of the paper have the same atomic arrangement as the Sb plane shown. If there is no surface reconstruction, the shadowing and blocking cone effects are expected to be the same for both In (solid line) and Sb (dashed line, Fig. 9). The sharp minima labelled *a* and *c* (Fig. 9-I) occur at angles corresponding to self-shadowing of In by In and Sb by Sb. Additional small fluctuations are believed due to blocking effects which require further study. If oxygen adsorbs at vacant sites in the extended lattice, then there will be a variation in intensity but not in the positions of the minima. In order to observe effects due to the preferential adsorption of oxygen, we take the Sb/In ratio as shown in Fig. 9-II. From the observed shadowing and blocking angles, we can verify the possible adsorption sites. Minima *a*

and *c* correspond to 0° and 45° angles between the incident beam and the normal to the surface, while *b* and *d* correspond to 0° and 45° angles between the scattered beam and the normal to the surface. The observed minima therefore correspond to a model in which the oxygen atoms are preferentially adsorbed on the empty Sb sites formed by the extension of the InSb lattice into the vacuum region adjacent to the surface, resulting in the minima *a* and *c* by shadowing, and *b* and *d* by blocking effects.

Figure 10 (top) shows the two possible arrangements of In and Sb atoms in the (110) plane perpendicular to the (001) surface. The two configurations shown have equal probability. Along the [110] azimuth, In and Sb atoms shadow and block each other. The ARISS data along the [110] azimuth show that the In and Sb signals are nearly identical in magnitude, indicating that the surface was terminated by about 50% In atoms and 50% Sb atoms as expected. Figure 10 (bottom) shows the ARISS results along [110] azimuth before and after oxygen exposure for the Sb intensity (the In intensity fluctuation is identical and not shown). The observed intensity minima are consistent with the assignment of the [001], [113], [112], [111] directions to the minima *a, b, c, d*, respectively. Based on this assignment, we calculated the vertical layer spacings of the first five layers (Table 1). Comparing these data to the lattice spacing of bulk InSb, we determined that the sputtered-cleaned (001) InSb surface undergoes a contraction between the first and second layer of about 0.6Å, and a contraction between the second and fifth layer of 0.9Å. After one monolayer of oxygen adsorption, the contraction between the first and second layer is relaxed completely, while the contraction between the second and fifth layer is relaxed by 50% as shown in Table 1.

IV. SUMMARY

The data presented here demonstrate the use of in situ, real time ISS analysis as a unique method of characterizing the growth of very thin Pb, Ru, and Zr layers, both in UHV and at pressures up to 0.5 mTorr, at temperatures relevant to the growth of complex oxides such as PZT. Modes of growth (layer-by-layer vs island), segregation, and oxygen stabilization phenomena were observed under thin-film growth conditions. In the case of the ultrathin-film growth study, we observed that Pb grows layer-by-layer, both at room temperature in UHV and below 420°C in an oxygen atmosphere of 5×10^{-4} Torr. Ru also grows in a layer-by-layer fashion for doses exceeding the equivalent of one monolayer. For lower Ru coverage on Pb, atomic interchange between the first two atomic layers produces a surface layer which is nearly entirely Pb. The study of oxygen adsorption on (001) InSb epitaxial films demonstrates the capabilities of in situ TOF-ISS as a powerful tool for gas adsorption and surface structural analysis. It was found that oxygen adsorption on the InSb (001) surface is consistent with the Langmuir model, with oxygen preferentially adsorbing on empty Sb sites in the extended lattice. For an oxygen-free surface, the

interatomic spacing between the first five alternating In and Sb layers is contracted relative to the bulk layer spacing. Adsorption of oxygen restores the bulk lattice spacing for the first two atomic layers and increases the spacing for layers 2-5 to a value intermediate between the bulk and the clean surface values.

ACKNOWLEDGMENTS

We thank Linqian Qian in the Materials Science Department, Northwestern University, for the InSb thin-film preparation. This work has been supported by the U. S. Department of Energy, BES-Materials Sciences, under contract W-31-109-ENG-38, as part of a cooperative research and development agreement between Argonne National Laboratory and the Ionwerks Corporation; and the Advanced Research Programs Agency under Grant N00014-93-1-0591.

REFERENCES

1. J. W. Rabalais, Science, **250**, 521 (1990).
2. H. Niehus and R. Spitzl, Surf. & Inter. Analysis, **17**, 287 (1991).
3. M. Aono, R. Souda, Jpn. J. Appl. Phys., **24**, 1249 (1985).
4. H. N. Al-Shareef, K. R. Bellur, O. Auciello, and A. I. Kingon, Proc. 8th Intl. Meeting on Ferroelectricity, Gaithersburg, MD, September 1993 (in press 1993).
5. D. J. Lichtenwalner, R. Dat, O. Auciello, and A. I. Kingon, Proc. 8th Intl. Meeting on Ferroelectricity, Gaithersburg, MD, September 1993 (in press 1993).
6. R. Ramesh, H. Gilchrist, T. Sand, V. G. Keramidas, R. Haakenaasen, and D. K. Fark, Appl. Phys. Lett., (in press 1993).
7. J. L. Davis, P. E. Thompson, Appl. Phys. Lett., **54**, 2235 (1989).
8. G. E. Franklin, D. H. Rich, H. Hong, T. Miller, and T.-C. Chiang, Phys. Rev., **B45**, 3426 (1992).
9. M. O. Schweitzer, F. M. Leibsle, T. S. Jones, C. F. McConville, and N. V. Richardson, Surf. Sci., **280,** 63 (1993).
10. C. E. C. Wood, K. Singer, T. Ohashi, L. R. Dawson, and A. J. Noreika, J. Appl. Phys., **54**, 2732 (1983).
11. S. D. Evans, L. L. Cao, R. G. Egdell, R. Droopad, S. D. Parker, and R. A. Stradling, Surf. Sci., **226**, 169 (1990).
12. J. F. Klem, J. Y. Tsao, J. L. Reno, A. Datye, and S. Chadda, J. Vac. Sci. Technol., **A9**, 2996 (1991).
13. A. R. Krauss, M. Rangaswamy, Y. Lin, D. M. Gruen, J. A. Schultz, H. K. Schmidt, and R. P. H. Chang, "Ion Beam-Based Characterization of Multicomponent Oxide Thin-Films and Thin-Film Layered Structures," in Multicomponent and Multilayered Thin Films for Advanced Microtechnologies: Techniques, Fundamentals and Devices, NATO/ASI Book Series E234, O. Auciello and J. Engemann, eds., Kluwer Academic Publishers, The Netherlands, 1993, p. 251.
14. A. R. Krauss, Y. Lin, O. Auciello, G. J. Lamich, D. M. Gruen, J. A. Schultz, K. Waters, and R. P. H. Chang, 40th National AVS Symposium, Orlando, FL, November 15-19, 1993.
15. O. Auciello, L. Mantese, J. Duarte, X. Chen, S. H. Rou, A. I. Kingon, A. F. Schreiner, and A. R. Krauss, J. Appl. Phys., **73**, 5197 (1993).
16. A. R. Krauss and O. Auciello, U.S. Patent #4, 923, 585 (1990).
17. A. R. Krauss, O. Auciello, A. I. Kingon, M. S. Ameen, Y. L. Liu, T. Barr, T. M. Graettinger, S. H. Rou, C. S. Soble, and D. M. Gruen, Appl. Surf. Sci., **46**, 67 (1990).
18. L. Qian, B. W. Wessels, Appl. Phys. Lett., **63**, 628 (1993).
19. A. R. Krauss, D. M. Gruen, and A. B. DeWald, J. Nucl. Mater., **121**, 398 (1984).

REFERENCES (contd.)

20. R. C. Sharma, T. L. Ngai, and Y. A. Chang, "In-Sb," Phase Diagram of Indium Alloys and Their Engineering Applications, C. E. T. White, and H. Okamoto, eds., ASM International, Metals Park, OH, p. 233 (1992).
21. J. B. Wachtman and R. A. Haber, "Ceramic Films and Coatings," Noyes Publications, Park Ridge, NJ, p. 4 (1993).
22. V. F. Kiselev and O. V. Krylov, "Adsorption Processes on Semiconductor and Dielectric Surface I," Springer-Verlag Publications, New York, p. 162 (1976).
23. J. P. McKelvey, "Solid State and Semiconductor Physics," Harper & Row Publishers, New York, p. 10 (1966).

Table 1

Atomic layer spacing of the (001) InSb surface caculated from ISS shadowing.

		[113] $d_{2\text{-}5}$	[112] $d_{1\text{-}5}$	[111] $d_{1\text{-}2}$
bulk	angle	25.54°	35.26°	54.74°
	layer spacing d_b (Å)	4.86	6.48	1.62
clean surface	angle	30°	42.5°	65°
	layer spacing d_{cs} (Å)	3.97	5.00	1.07
	contraction d_b-d_{cs} (Å)	0.89	1.48	0.55
O exposed surface	angle	27.5°	37.5°	55°
	layer spacing d_{os}(Å)	4.40	5.97	1.6
	contraction d_b-d_{os} (Å)	0.46	0.51	0.02

Table 1

Atomic layer spacing of the (001) InSb surface caculated from ISS shadowing.

		[113] $d_{2\text{-}5}$	[112] $d_{1\text{-}5}$	[111] $d_{1\text{-}2}$
bulk	angle	25.54°	35.26°	54.74°
	layer spacing d_b (Å)	4.86	6.48	1.62
clean surface	angle	30°	42.5°	65°
	layer spacing d_{cs} (Å)	3.97	5.00	1.07
	contraction d_b-d_{cs} (Å)	0.89	1.48	0.55
O exposed surface	angle	27.5°	37.5°	55°
	layer spacing d_{os}(Å)	4.40	5.97	1.6
	contraction d_b-d_{os} (Å)	0.46	0.51	0.02

FIGURES

Fig. 1 Differentially pumped ISS/DRS, AES, XPS chamber and ion beam thin-film deposition chamber.

Fig. 2. 10 keV Ar^+ ISS spectra of Pb and Ru deposition: (a) before deposition, (b) after 3.7 Å Pb deposition, (c) after 1.2 Å Ru deposition on the top of Pb, and (d) after 2.9 Å Ru deposition.

Fig. 3. Pb and Ru ISS intensity variation as a function of the Pb deposition time.

Fig. 4. In situ, real-time 10keV Ne^+ ISS spectra of Pb deposition onto a Zr-covered RuO_2 layer on a MgO (100) substrate in an atmosphere of $5X10^{-4}$ Torr oxygen at a substrate temperature of 420°C.

Fig. 5. AES spectra of InSb (001) surface: (a) before cleaning, (b) after 60 minutes of 10^{-6} Torr oxygen exposure, and (c) after 18 hours at 10^{-9} Torr.

Fig. 6. The O(KLL) Auger intensity I and $\ln(I_S-I)$, where I_S is the saturated intensity as a function of oxygen exposure.

Fig. 7. In situ ISS spectra in normal incidence during $1X10^{-6}$ Torr oxygen exposure. Successive spectra *a-g* correspond to an incremental exposure of 600 L.

Fig. 8. Sequential 10 keV Ar^+ ISS spectra of the oxygen covered (001) InSb surface during depth profile. Successive spectra correspond to incremental removal of approximately 0.5 ML.

Fig. 9. Sb (dashed line) and In (solid line) intensity and their ratio for 10keV Ar^+ incident on (001) InSb thin-film as a function of polar angle of incidence along the [010] azimuth after oxygen adsorption.

Fig. 10. Top: The layered structure of (001) InSb surface along the [110] azimuth. Bottom: Intensity of the Sb ISS line for 10keV Ar^+ incident on (001) InSb thin-film as a function of polar angle of incidence along the [110] azimuth for clean (solid line) and oxygen-covered (dashed line) surfaces. The minima labelled a-a', b-b' c-c' and d-d' correspond to the [001], [113], [112], and[111] directions, respectively.

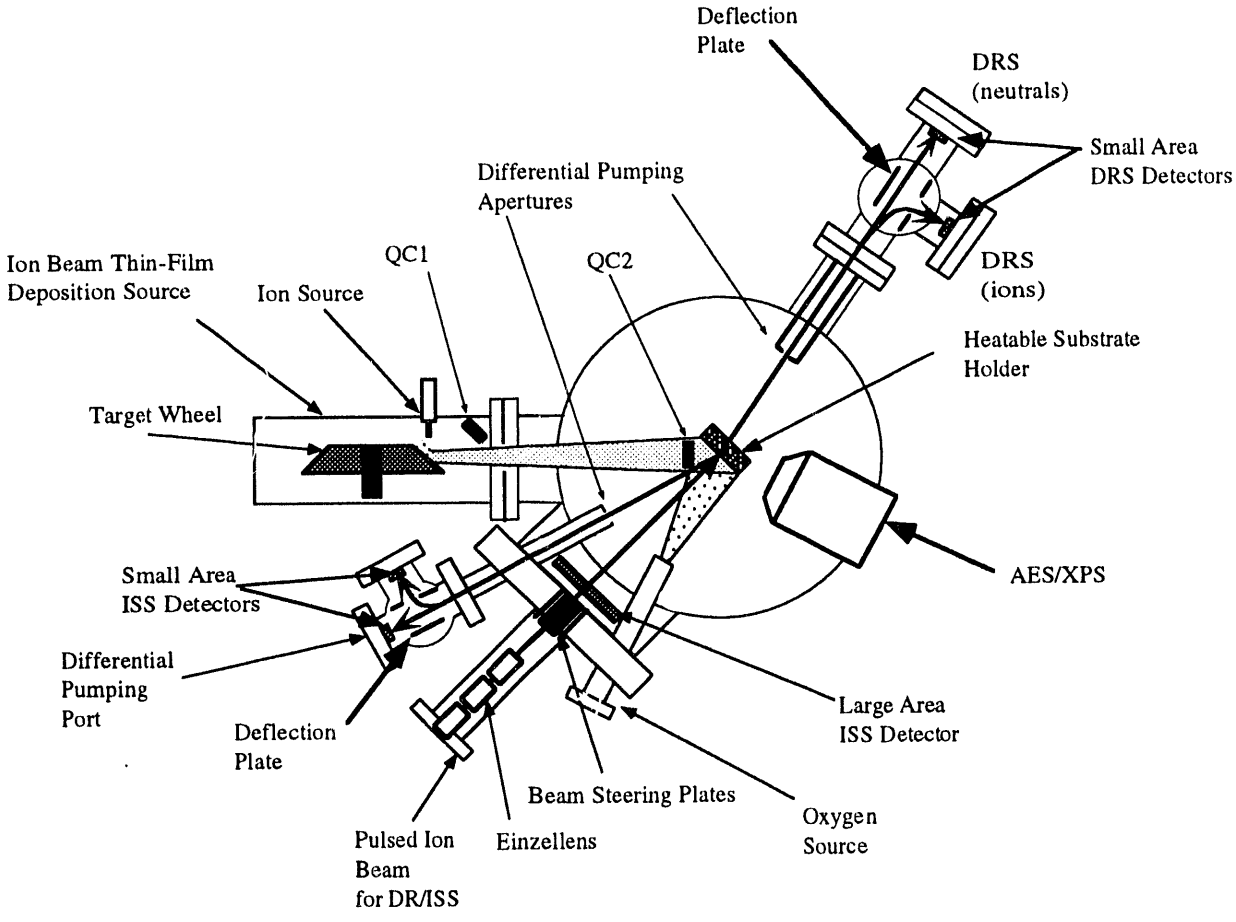

Lin et al Fig 1

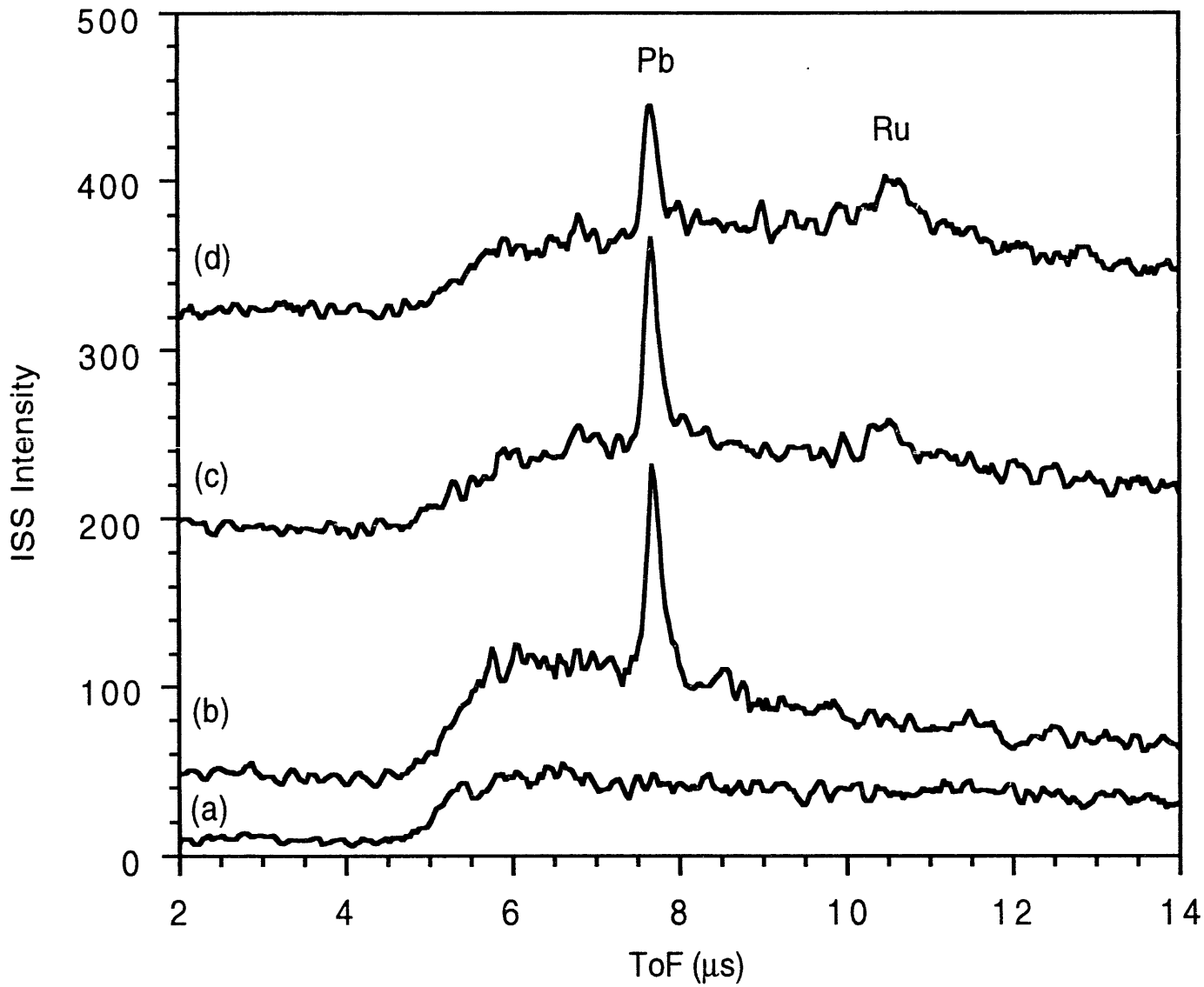

Lin et al. Fig. 2

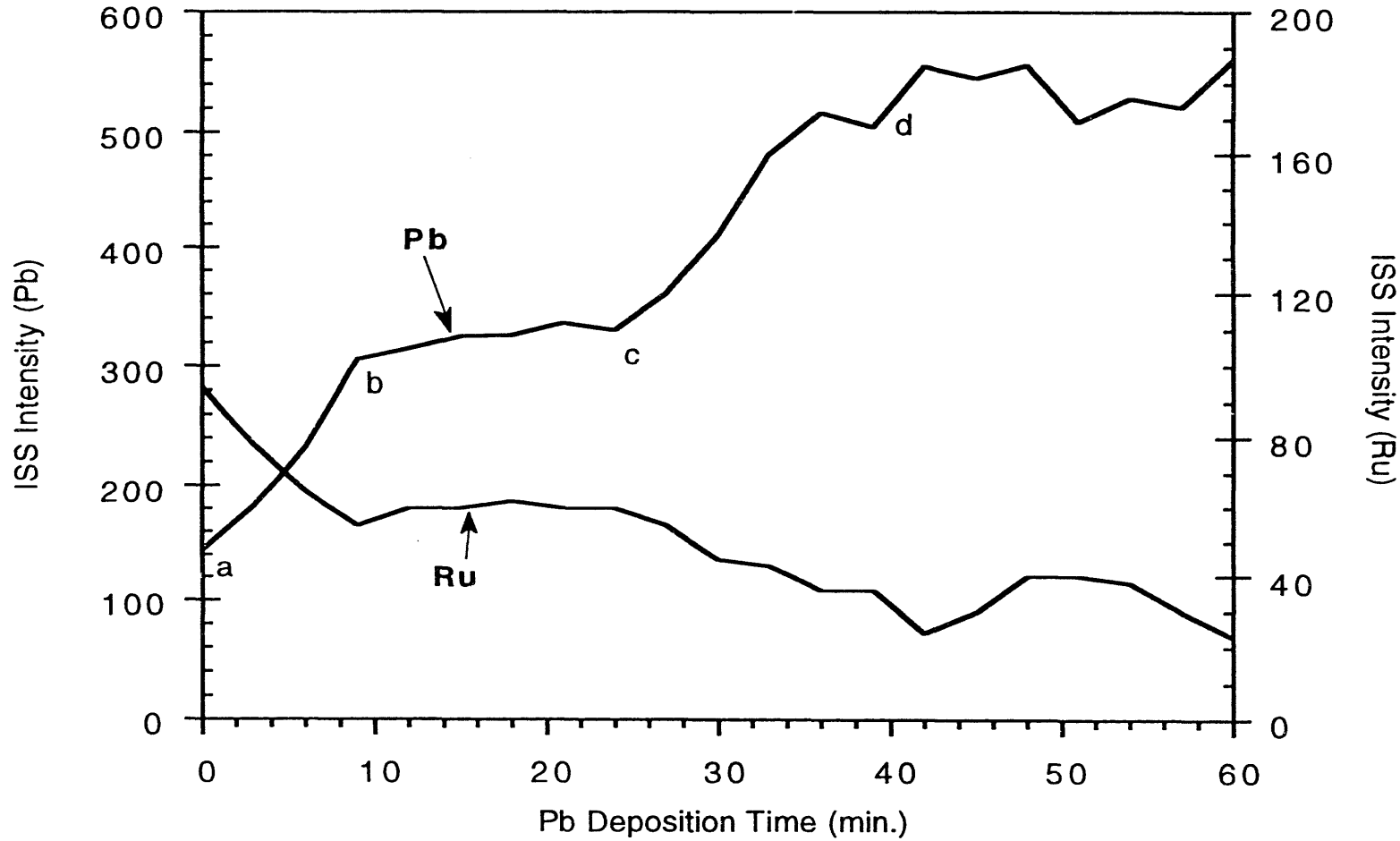

Lin et. al. Fig. 2

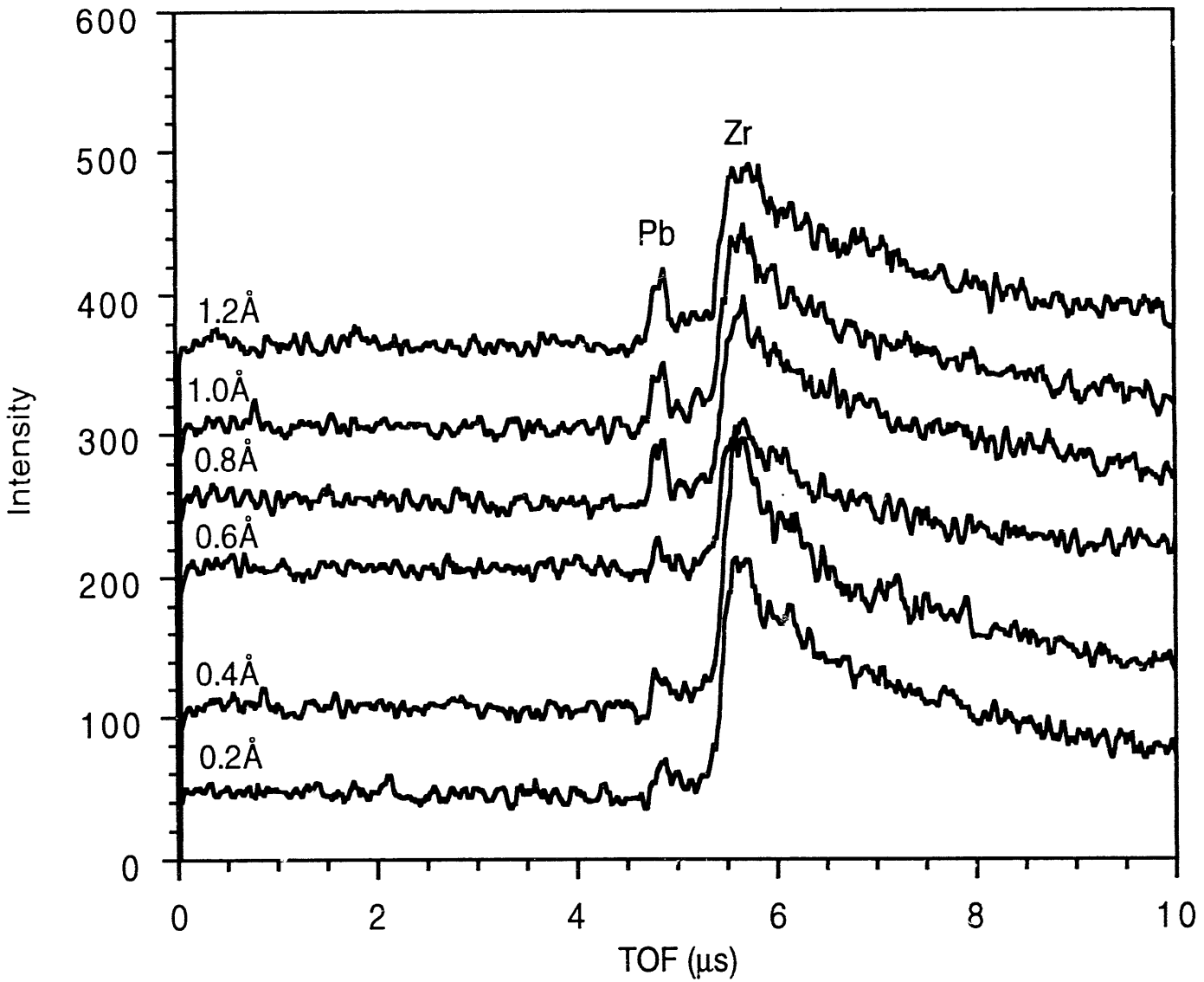

Lin et.al. Fig. 4

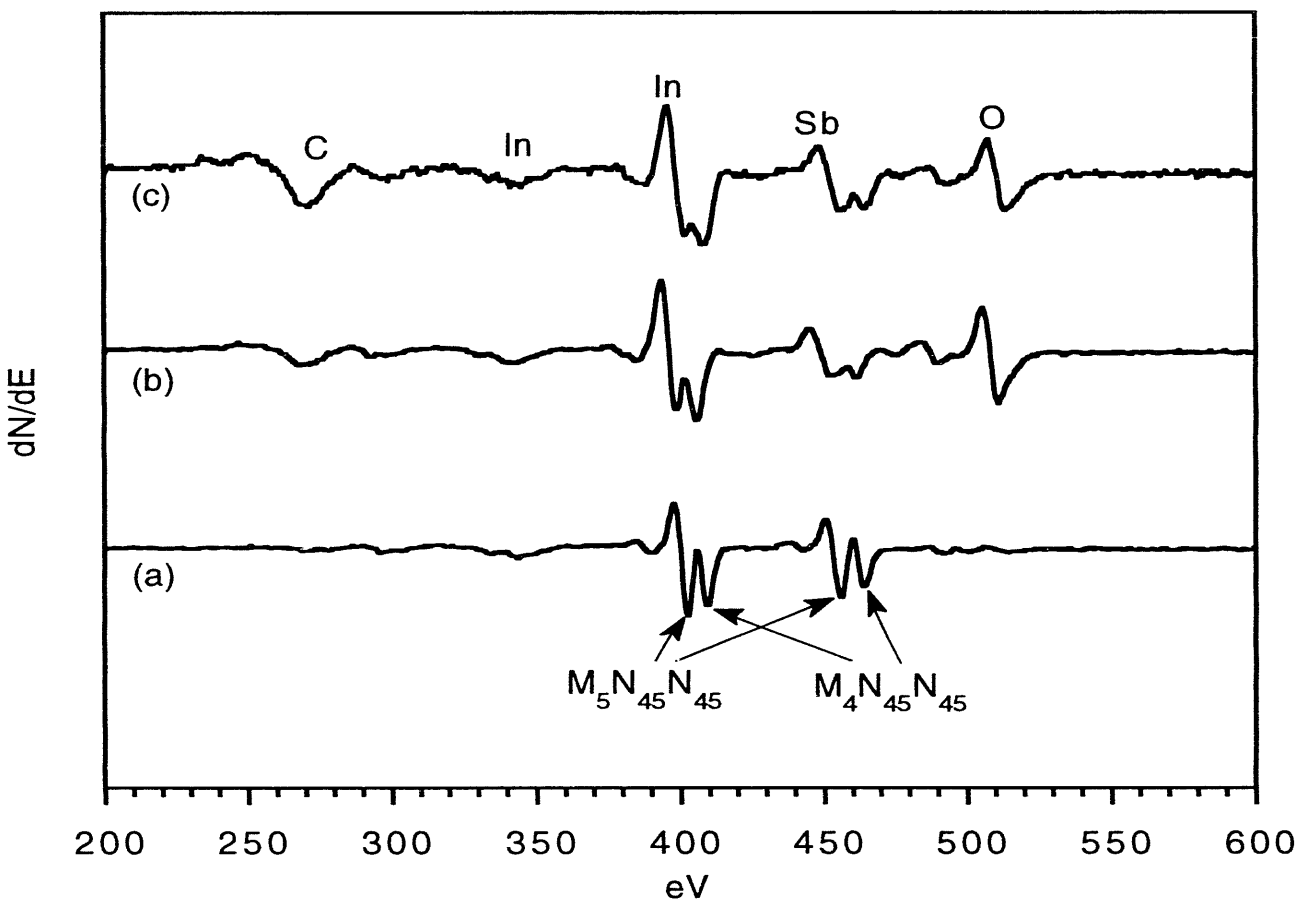

Lin et. al. Fig 5

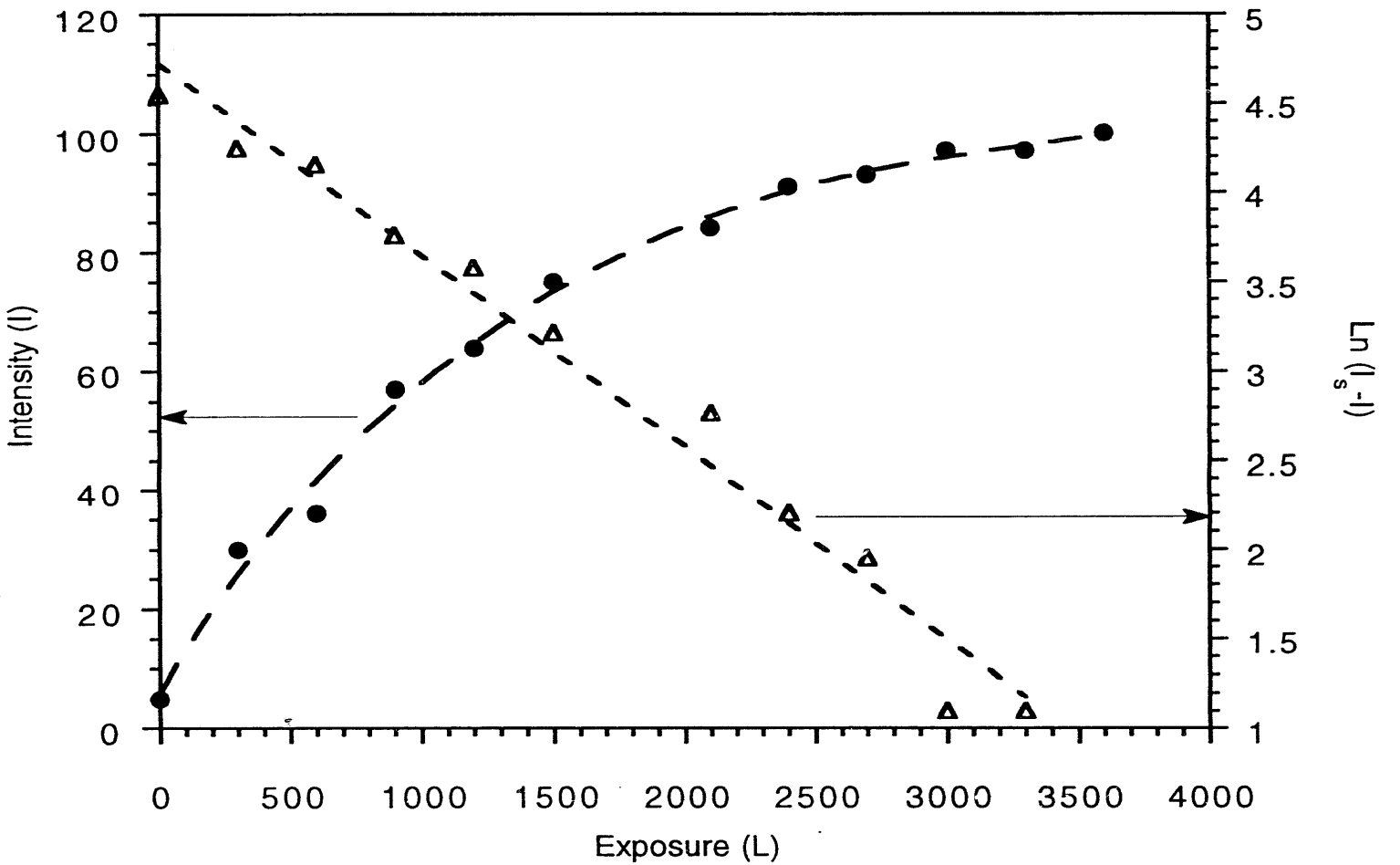

Lin et. al. Fig. 6

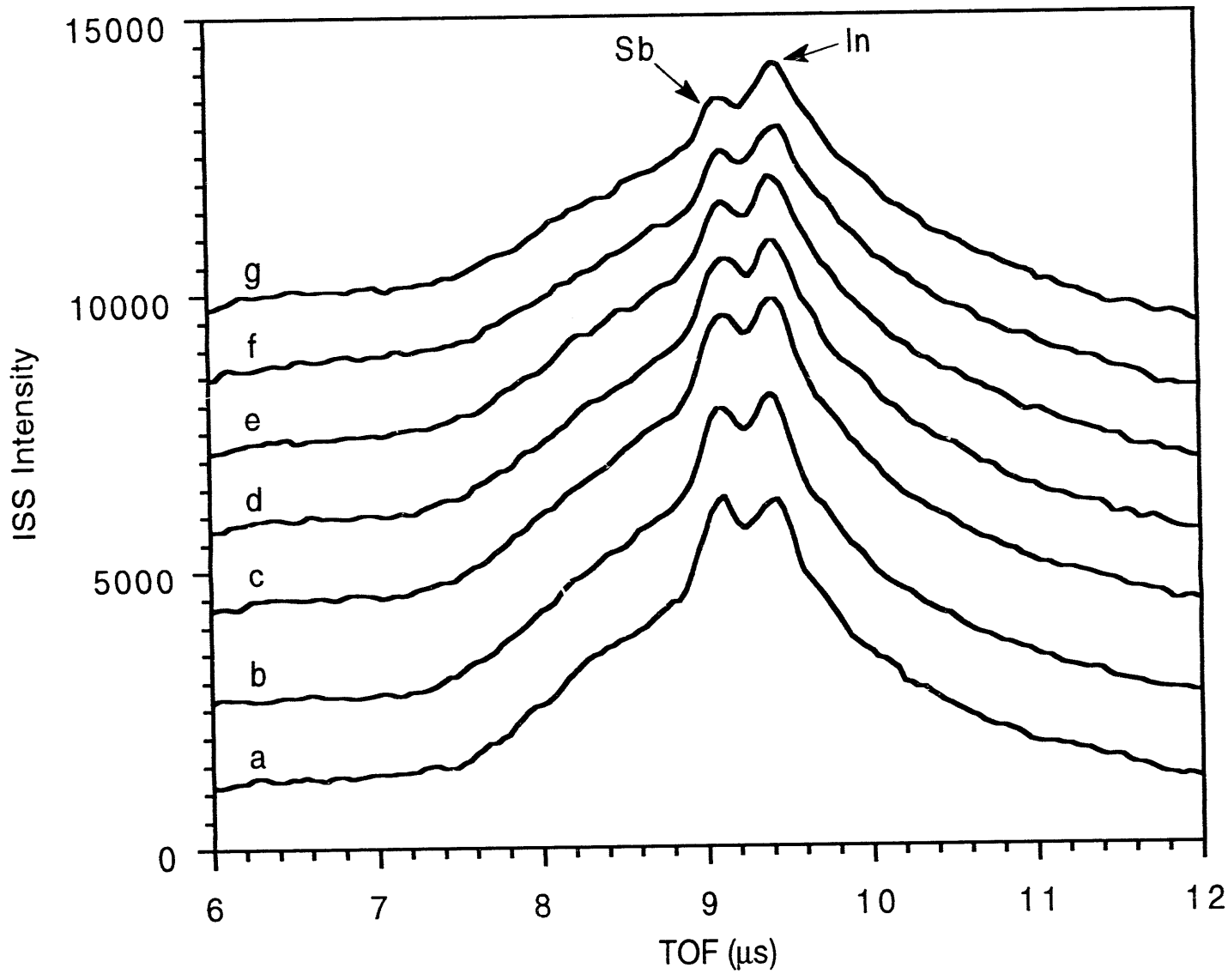

Lin et. al. Fig 7.

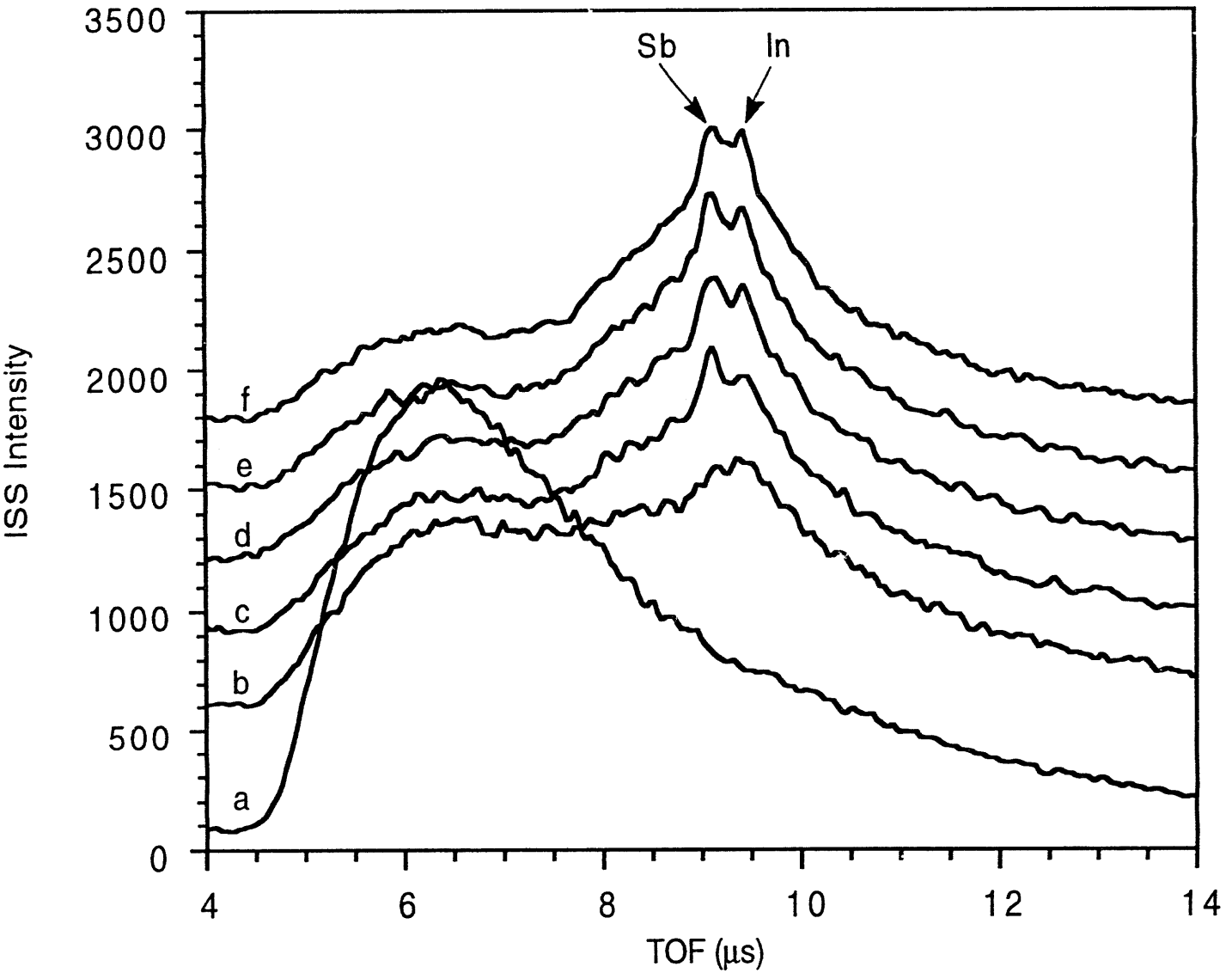

Lin et al Fig 8.

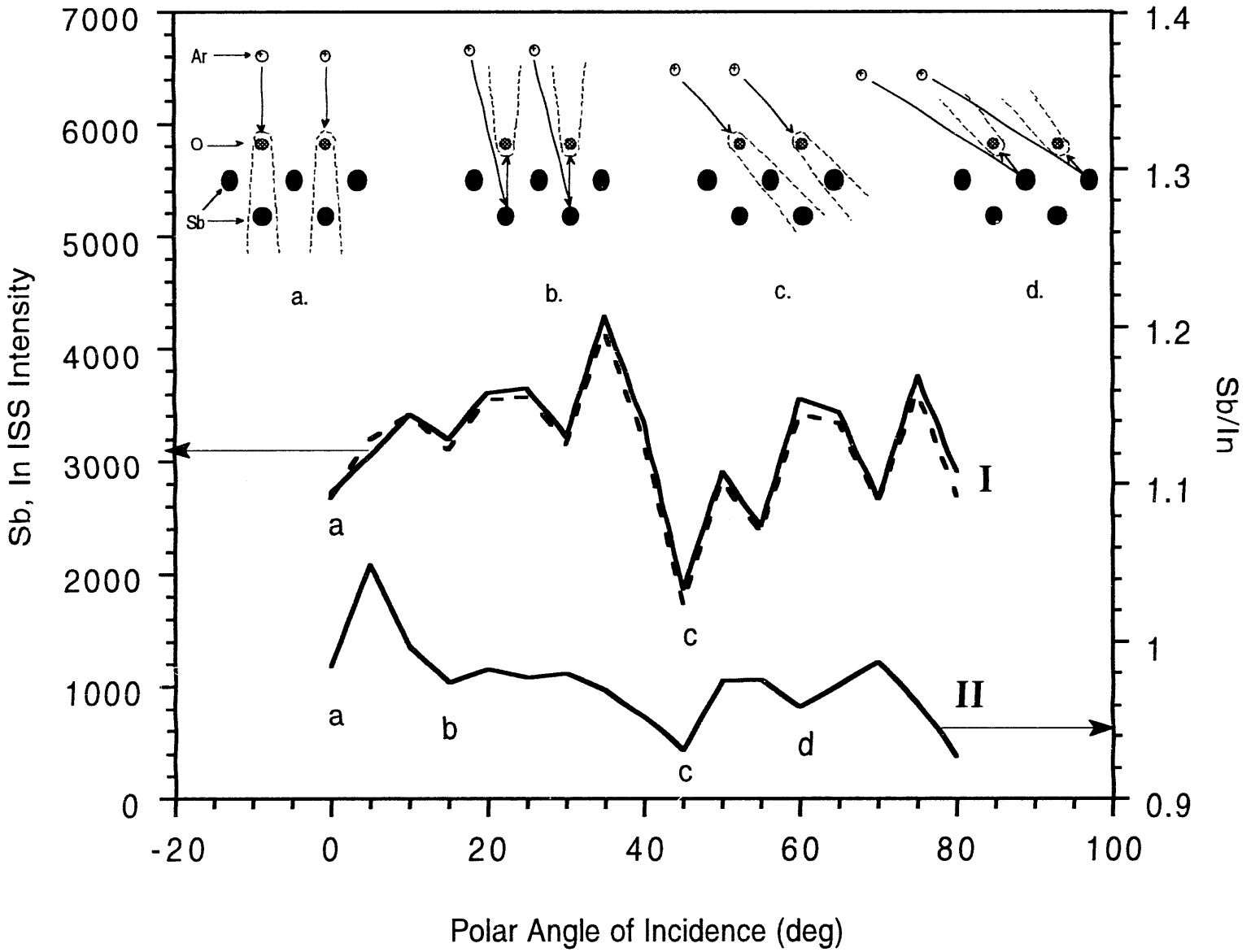

Lin et.al. Fig. 9

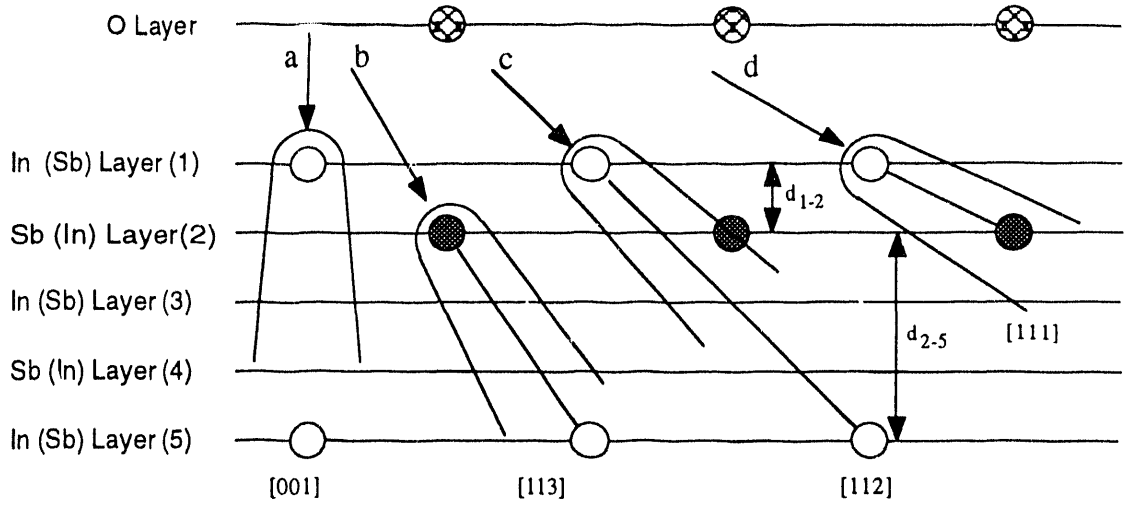

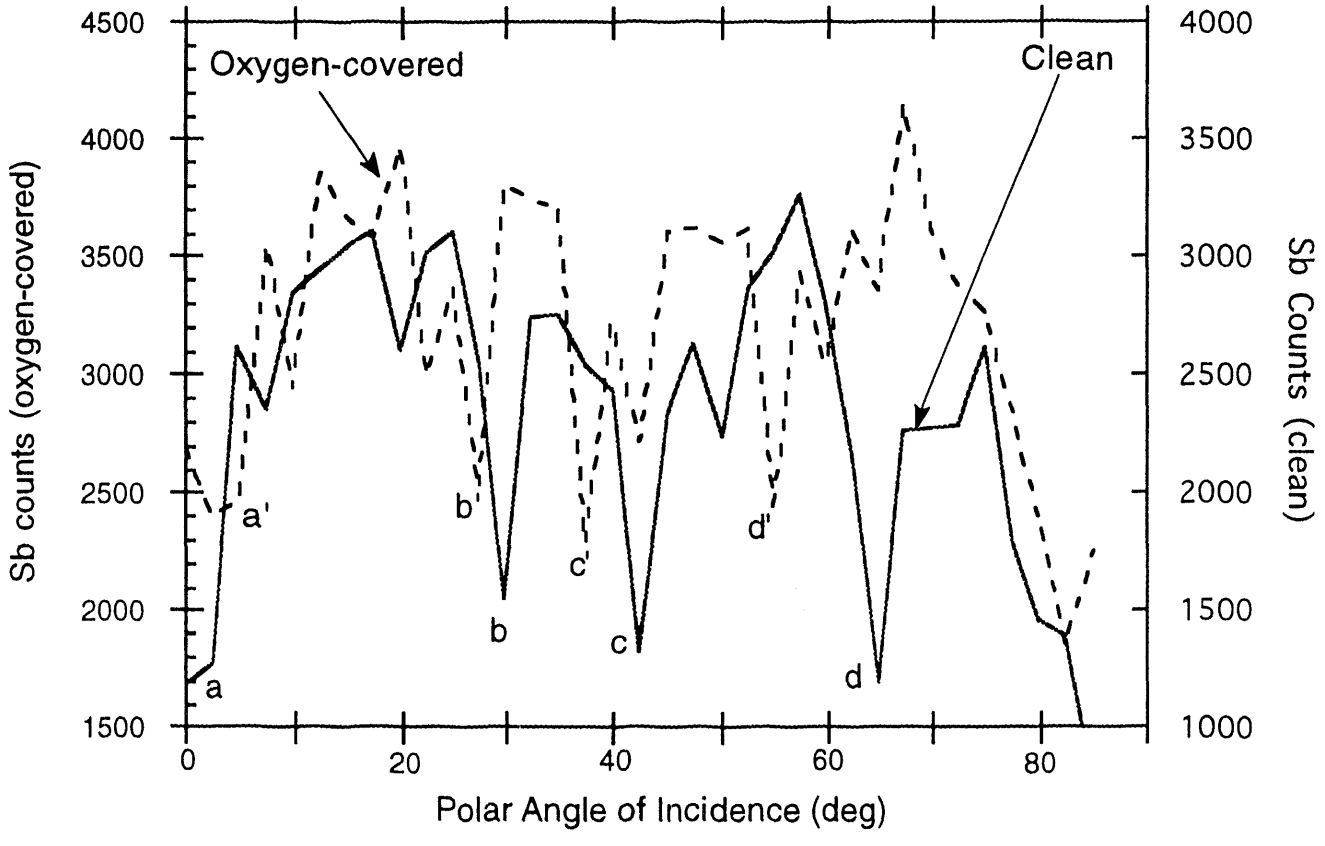

Lin et. al. Fig. 10

DATE
FILMED
1/11/94
END